HHS Public Access

Author manuscript

J Immunol. Author manuscript; available in PMC 2025 January 01.

Published in final edited form as:

J Immunol. 2024 January 01; 212(1): 24–34. doi:10.4049/jimmunol.2200956.

Distinct functional humoral immune responses are induced after live attenuated and inactivated seasonal influenza vaccination

Xin Tong[*,§], **Yixiang Deng**[*,§], **Deniz Cizmeci**[*], **Laura Fontana**[*], **Michael A. Carlock**[†], **Hannah B. Hanley**[†], **Ryan P. McNamara**[*], **Daniel Lingwood**[*], **Ted M. Ross**[†,‡], **Galit Alter**[*]

[*]Ragon Institute of MGH, MIT, and Harvard, Cambridge, MA, USA.

[†]Center for Vaccines and Immunology, University of Georgia, Athens, GA, USA

[‡]Department of Infectious Diseases, University of Georgia, Athens, GA, USA

Abstract

Influenza viruses infect 5–30% of the world's population annually, resulting in millions of incidents of hospitalization and thousands of mortalities worldwide every year. While annual vaccination has significantly reduced hospitalization rates in vulnerable populations, the current vaccines are estimated to offer a wide range of protection from 10–60% annually. Such incomplete immunity may be related to both poor antigenic coverage of circulating strains, as well as to the insufficient induction of protective immunity. Beyond the role of hemagglutination (HA) and neuraminidase (NA), vaccine-induced antibodies have the capacity to induce a broader array of antibody effector functions, including antibody-dependent cellular cytotoxicity, that has been implicated in universal immunity against Influenza viruses. However, whether different vaccine platforms can induce functional humoral immunity in a distinct manner remains incompletely defined. Here, we compared vaccine-induced humoral immune responses induced by two seasonal influenza vaccines in *Homo Sapiens*, the intramuscular inactivated vaccine (IIV/FluZone) and the live attenuated mucosal vaccine (LAIV/FluMist). While the inactivated influenza vaccine induced superior antibody titers and Fcγ-receptor binding capacity to diverse HA and NA antigens, the live attenuated influenza mucosal vaccine induced a more robust functional humoral immune response against both the HA and NA domains. Multivariate antibody analysis further highlighted the significantly different overall functional humoral immune profiles induced by the two vaccines, marked by differences in IgG titers, FcR binding, and both NK cell-recruiting and opsinophagocytic antibody functions. These results highlight the striking differences in antibody Fc-effector profiles induced systemically by two distinct influenza vaccine platforms.

C*orresponding authors*: Galit Alter. galter@partners.org. Phone number: 857-268-7003. Fax = 857-268-7142.
[§]Contributed equally.

Declarations of Interests

GA is a founder/equity holder in Seroymx Systems. GA is an equity holder in Leyden Labs. GA has served as a scientific advisor for Sanofi Vaccines. GA has held collaborative agreements with GSK, Merck, Abbvie, Sanofi, Medicago, BioNtech, Moderna, BMS, Novavax, SK Biosciences, Gilead, and Sanaria. GA is an employee of Moderna. TMR serves on the scientific advisory board of TFF Pharma and Centivax and has held collaborative agreements with Sanofi Pasteur, Medicago, Novavax, Moderna, Gritstone Bio, Inimmune, Dynavax, Centivax, and PDS Biotechnologies.

Keywords

antibody; influenza; Fc receptor; placental transfer; vaccination; Fc effector function

Introduction

Despite decades of research and the development of multiple seasonal vaccines, the influenza virus remains an important global public health concern. This is owed to its ability to escape pre-existing immunity from prior circulating strains, as well as causing seasonal epidemics and numerous pandemics (1–3). Seasonal influenza vaccines have repeatedly shown incomplete real-world vaccine effectiveness due to circulating strain mismatch, rapid, unpredictable mutations in the virus, or poor immunogenicity in vulnerable populations (4). Yet, even when the vaccine is well-matched, vaccine effectiveness has only reached 10–60% (2), suggesting that other immunologic parameters, beyond the strain sequence matching, including the quality of the vaccine-induced immune responses, are likely to be critical for driving population level immunity against influenza (5).

Antibody-mediated hemagglutinin agglutination inhibition (HAI), a surrogate activity of viral neutralization, represents the primary correlate of protection against influenza infections (6). However, universally protective influenza-specific monoclonal antibodies that provide the broadest level of protection across viral strains confer protection in a neutralization-independent manner. Rather, these protective antibodies mediate the recruitment of the innate immune response through antibody constant domain (Fc) and Fc-receptor interactions (7). Likewise, emerging data point to a critical role for antibody-dependent cellular cytotoxicity (ADCC), antibody-dependent cellular phagocytosis (ADCP), and antibody-dependent complement activation (ADCD) in overall protection against influenza (5). However, whether any specific seasonal influenza vaccines are capable of promoting such functional activities more efficiently than others remains incompletely understood.

Several influenza vaccines are currently approved and globally deployed including the intramuscular inactivated influenza virus (IIV/FluZone) and the mucosal replication-competent live attenuated influenza vaccine (LAIV/FluMist) (3). Previous studies have demonstrated that compared to IIV/FluZone, LAIV/FluMist induced comparable serum neutralizing antibody responses, quantified using the HAI assay, but demonstrated significantly higher T cell responses in young children than IIV/FluZone (8). Conversely, in adults, LAIV/FluMist induced only moderate increases in serum antibody responses, much lower than those induced by IIV/FluZone (9), but induced higher virus-specific secretory IgA (10). Differences in adult responsiveness, compared to children have been attributed to the potential role of pre-existing immunity that may attenuate the ability of the vaccine virus to replicate within the respiratory tract (11). However, despite these differences in HAI, little is known about the ability of these two vaccine platforms to promote antibody effector functions and how they are modulated by pre-existing immunity.

Thus, given our emerging appreciation for the role of Fc-associated functions in protection against virus-driven diseases, we aimed to profile the functional humoral immune

responses induced by both IIV/FluZone and LAIV/FluMist vaccines. We hypothesized that these vaccines drive distinct antibody functional profiles due to the different routes of administration and susceptibility to pre-existing immunity. Using the previously established systems serology platform, we profiled the Fc-profiles induced by IIV/FluZone and LAIV/FluMist against a panel of influenza hemagglutinin (HA) and neuraminidase (NA) antigens (12), including both contemporaneous antigens, as well as historical, future, and computationally derived influenza antigens. Distinct profiles of influenza-specific antibody profiles and functions were observed between the two vaccine platforms, with IIV/FluZone inducing significantly higher antibody titers and Fc-receptor-binding capabilities. Conversely, LAIV/FluMist promoted higher levels of antibody-dependent cell functions across various influenza strains, particularly against the NA component. These results present the first comprehensive functional and humoral comparison between the two types of influenza vaccines and provide insights underlying the comparable protection observed by these two influenza vaccines despite their striking differences in serological immunogenicity.

Materials and Methods

Samples

As part of an ongoing study by the University of Georgia, Athens (UGA), the participants studied in this manuscript received either the split-inactivated influenza vaccine Fluzone by Sanofi Pasteur (IIV/FluZone, n = 63) or the live attenuated influenza vaccine (LAIV) by MedImmune delivered as an intranasal spray (LAIV/FluMist, n = 94). The study procedures, informed consent, and data collection documents were reviewed and approved by the Institutional Review Board of the University of Georgia (IRB #3773). During the 2018–2019 season, the same influenza strains included in the vaccine formulation of both the IIV/FluZone and LAIV/FluMist vaccines were as follows: A/Michigan/15 (H1N1), A/Singapore/16 (H3N2), B/Phuket/2013 (Yamagata lineage), and B/Colorado/2017 (Victoria lineage). The serum samples were collected in collaboration with UGA's Clinical and Translational Research Unit (CTRU) which oversees patient recruitment, vaccinations, and sample collections. Serum samples were collected at Day 0 followed by vaccination with the Northern Hemisphere (NH) seasonal influenza vaccine. Second serum samples were collected on Day 28 post-vaccination to evaluate the vaccine-induced antibody responses. Participants who received the IIV/FluZone vaccine in this study were described in a previous publication (13). Participants who received the LAIV/FluMist vaccine in this study have not be published previously to our knowledge. The detailed information regarding the composition of populations of the two subgroups including gender, age, BMI, race, and the previous history of influenza vaccination, is provided in Table S1 as part of Supplementary Information. Statistical analyses were performed on these additional confounders to evaluate whether the two subgroups are statistically different in terms of their gender, age, race, BMI, and previous history of influenza vaccination. The detailed results of such comparison are summarized in Table 1.

Ig Subclassing/Isotyping and FcR binding

Antigen-specific antibody subclass/isotypes and FcR binding were determined using a high-throughput Luminex-based assay (14, 15). Antigens included were: H1 A/California/07/2009, H3 A/Perth/16/2009, HA B/Brisbane/60/2008, H3 A/Victoria/361/2011, HA B/Wisconsin/01/2010, H3 A/Singapore/INFIMH-16–0019/2016, HA B/Colorado/06/2017, H1 A/New Caledonia/1999, H3 A/Wisconsin/67/X-161/2005, HA B/Malaysia/2506/2006, all provided from Immune Technology Corp., and EBOV GPdTM from Mayflower Bioscience, St. Louis, MO. Bolded strains indicate vaccine strains during the trial. Antigens were coupled to carboxylate-modified microspheres (Luminex Corp., Austin, TX) by covalent NHS-ester linkages via EDC (ThermoFisher) and Sulfo-NHS (ThermoFisher) per manufacturer's instructions. These antigen-coated microspheres were added to non-binding 384-well plates (Grenier Bio-One, Kremsmunster, Austria) at 1000 beads per well (45 µl). Serum samples were diluted at 1:100 for IgG1, total IgG, and FcRs, and 1:10 for IgG2–4, IgA1–2, and IgM prior to incubation with beads. 5 µl of diluted serum samples were added and incubated with microspheres on a shaker overnight at 4°C. Microspheres were washed, and PE-conjugated anti-IgG1, -IgG2, -IgG3, -IgG4, -IgG, -IgM, -IgA1, or -IgA2 detection antibodies (Southern Biotech, Birmingham, AL) or biotinylated FcRs (Duke University Protein Production Core) conjugated to streptavidin-PE (Prozyme, Hayward, CA) were added for 1 hour at room temperature. The microspheres were washed and read on an iQue Screener Plus. All samples were run in duplicate and correlation between duplicates was ensured. Data are reported as the median fluorescence intensity (MFI) of the detection antibody for the average of two replicates.

Antibody-dependent cellular phagocytosis (ADCP)

THP-1 phagocytosis of HA-coated beads was performed as previously described (16). HA antigens (H1 A/California/07/2009, H3 A/Perth/16/2009, H3 A/Victoria/361/2011, HA B/Wisconsin/01/2010, and HA B/Brisbane/60/2008) were purchased from Immune Technologies Corp, New York, NY. Each recombinant antigen was biotinylated with EZ-link NHS-LC-LC Biotin per the manufacturer's instructions (Thermo Fisher Scientific). Biotinylated protein was adsorbed onto fluorescent neutravidin beads at a ratio of 10 µg of protein to 10 µl of beads (Invitrogen, Carlsbad, CA). 10 µL of antigen-coated beads were then incubated with an equal volume of serum samples diluted 1:200 in PBS for 2 hours at 37°C in 96-well plates. Unbound antibody was washed away, and THP-1 cells were added and incubated at 37°C for 16 hours, then fixed. Phagocytosis was measured by flow cytometry on an iQue Screener Plus (IntelliCyt, Albuquerque, NM). Data are reported as phagocytic scores, calculated as the % of bead positive cells geometric mean fluorescence intensity (GMFI)/1,000. Each experiment was performed in two independent replicates and correlation between replicates was ensured.

Antibody-dependent neutrophil phagocytosis (ADNP)

Primary human neutrophil phagocytosis was performed as previously described (17). HA-coated 1 µm fluorescent neutravidin beads were prepared and incubated with equal volume 1:50 diluted serum samples as in the ADCP assay. Primary human leukocytes were isolated from healthy donors using Ammonium-Chloride Potassium (ACK) lysis, then added to

the opsonized beads and incubated at 37°C for 1 hour. The cells were then stained with fluorescent anti-human CD66b (Biolegend, San Diego, CA) and fixed prior to analysis on an iQue Screener Plus. Data are reported as phagocytic scores, calculated as the % of bead-positive CD66+ cells GMFI/1,000. Each sample was assayed on two healthy PBMC donors and correlation between donors was ensured.

Antibody-dependent complement deposition (ADCD)

Serum samples were heat-inactivated at 56°C for 30 minutes and centrifuged to remove aggregates. Bead-based antibody-dependent complement deposition was analyzed as previously described (18). The 5 HA molecules used for the ADCP and ADNP assays were pooled in equal amounts and adsorbed to 1 μm fluorescent neutravidin beads as in the ADCP assay. HA-coated beads were incubated with 1:25 diluted, heat-inactivated serum samples for 2 hours at 37°C. Lyophilized guinea pig complement (Cedarlane, Burlington, Canada) was resuspended in ice-cold water, then diluted at 1:60 in veronal buffer with calcium, magnesium, and gelatin (Boston Bioproducts, Ashland, MA). 150 μL diluted complement was added to the opsonized beads and incubated for 20 minutes at 37°C. Beads were then washed with 15 mM EDTA and stained with anti-guinea pig C3 (MP Biomedicals, Santa Ana, CA). Samples were washed and analyzed on an iQue Screener Plus. Each experiment was performed in two independent replicates and correlation between replicates was ensured. Data are reported as the GMFI of the C3 antibody for the average of two replicates.

Antibody-dependent NK Cell activation (ADNKA)

Antibody-dependent NK cell activation and degranulation were measured as previously described (19, 20). ELISA plates (ThermoFisher NUNC MaxiSorp) were coated with pooled HAs (as in ADCD), then blocked. 50 μL of 1:25 diluted serum sample was added to each well and incubated for 2 hours at 37 C. NK cells were isolated from buffy coats from healthy donors using the RosetteSep NK cell enrichment kit (STEMCELL Technologies, Vancouver, Canada) and rested in 1 ng/ml IL-15 at 37°C until needed. NK cells, with anti-CD107a PE-Cy5 (BD), brefeldin A (Sigma-Aldrich, St. Louis, MO), and GolgiStop (BD), were added and incubated for 5 hours at 37°C. Cells were stained for surface markers using anti-CD56 PE-Cy7 (BD), anti-CD16 APC-Cy7 (BD), and anti-CD3 PacBlue (BD), then fixed and permeabilized using FIX & PERM Cell Permeabilization Kit (ThermoFisher). Cells were stained for intracellular markers using anti-MIP1 PE (BD) and anti-IFN FITC (BD). Fixed cells were analyzed by flow cytometry on an iQue Screener Plus. NK cells were defined as CD3- and CD16/56+. Each sample was assayed on two healthy NK cell donors and correlation between donors was ensured. Further, each donor was independently quality controlled to ensure that positive control values were at least two standard deviations above negative control values. Data are reported as the percentage of cells positive for each marker (CD107a, IFN-ɣ, and MIP-1β).

Statistics and Computational Analyses

All data analysis was done using R Studio V 1.4.1103 or FlowJo. Statistical analysis was done using R studio or GraphPad Prism. No data point was omitted from the analysis. Box and whisker plots were generated using ggplot, calculating the mean and standard deviation

for each factor. Technical replicates for each sample were performed, and the mean between replicates was calculated and plotted.

In statistics, the z score value is the number of standard deviations by which the value of a raw score (i.e., Luminex MFI or phagocytic scores in this work) is above or below the mean value of what is being observed or measured. Raw values above the mean have positive z scores, while those below the mean have negative z scores. It is calculated by subtracting the population mean from an individual raw score and then dividing the difference by the population standard deviation.

Gating Strategy and Additional Materials

Flow cytometry gating strategy is shown in Figure S1. All flow cytometry experiments were conducted on the iQue Intellicyt using a 384-well high-throughput screener. Individual gates were generated using iQue Forecyt. Antigens, antibodies, and bead regions used are shown in Table S2 and S3.

Results

Univariate differences in antibody responses across LAIV/FluMist and IIV/FluZone.

Existing data point to significant differences in vaccine-induced immune responses between LAIV/FluMist and IIV/FluZone, including differences in neutralizing antibody titers, B and T cell activation, and vaccine effectiveness in different populations (11). However, despite the clear differences in IgA levels induced by these different platforms (21), the overall humoral landscape established by these vaccinations is unclear. Thus, we first probed the vaccination-induced antigen-specific antibody responses to the four commonly investigated H1, H2, and H3 and NA antigens, including A_California09_HA, A_California09_NA, A_Singapore16_HA, and B_Phuket13_HA in addition to an Ebola Glycoprotein control antigen. The antigen-specific influenza vaccine-induced responses were presented as fold increases between the post- (Day 28) and pre- (Day 0) vaccination titers (Figure 1). The results demonstrated that the level of enhancement in antibody titers induced by IIV/FluZone against multiple antigens were significantly higher than those by LAIV/FluMist, in line with previous studies (9). Neither vaccine induced a significant systemic IgA or IgM response. These results further confirm the previously proposed higher immunogenicity observed in the systemic circulation with IIV/FluZone compared to LAIV/FluMist.

IIV/FluZone induced more significant antigen-specific antibody binding to Fcγ-Receptors

Beyond vaccine-induced responses in antibody subclasses and isotype titers, we next aimed to determine whether the vaccines induced differential responses in the levels of the Fc-receptor (FcR) binding antibodies (Figure 2). We assessed the vaccination-induced antigen-specific responses in Fc-receptor (FcR) binding antibodies to the four H1, H2, and H3 and NA antigens, including A_California09_HA, A_California09_NA, A_Singapore16_HA, and B_Phuket13_HA in addition to an Ebola Glycoprotein control antigen. The antigen-specific influenza vaccine-induced improvement in receptor binding were presented as fold increases between the post- (Day 28) and pre- (Day 0) vaccination values. The results suggested that the levels of fold increases in antibodies binding to the opsinophagocytic receptor

FcγRIIA against A_California09_HA, A_California09_NA, and the A_Singapore16_HA induced by IIV/FluZone were significantly higher than those induced by LAIV/FluMist. A similar trend was also observed for the activating and cytotoxic FcγRIIIA-binding antibody responses, as IIV/FluZone induced a more profound improvement in the level of FcγRIIIA-binding antibodies against A_California09_NA, and A_Singapore16_HA than LAIV/FluMist. These data collectively suggest that the mucosal attenuated influenza vaccination may not significantly improve serum FcR binding profiles in influenza-specific antibodies to the same extent as the inactivated influenza vaccine.

We further assayed the same antibody parameters against an expanded library of antigens, including a series of influenza HA and NA antigens, in an attempt to expand our assessment of antibody functional responses beyond the common influenza antigens. In addition to the naturally circulating influenza variants, we further included a panel of the computationally derived recombinant influenza antigens in our Systems Serology assays. The computationally optimized broadly reactive antigens (COBRAs) are next-generation universal influenza vaccine candidates that incorporates wild-type HA or NA sequences from extended influenza epidemic periods and antigenic sequences to greatly expand the antigenic breadth (22–27). These COBRA antigens also represent both influenza A and B viruses. These previous studies demonstrated that CROBRA antigens were capable of eliciting broadly reactive antibodies that protect against seasonal and pandemic influenza virus strains. Therefore, the additional COBRA antigens could potentially expand the antigenic breadth of our profiling against the humoral responses induced by LAIV/FluMist and IIV/FluZone.

We observed a similar overall antibody profile to COBRA compared with the four antigens previously tested (Figure 3). Across the entire panel of antigens, IIV/FluZone displayed superior titer induction in total IgG, IgG3, and IgM over LAIV/FluMist. Furthermore, IIV/FluZone also promoted higher overall antibody responses in Fc-receptor binding to FcγRIIA and, less globally, to FcγRIIIA across the antigens. Interestingly, LAIV/FluMist vaccinees had increased FcγRIIB binding activities to multiple antigens, consistent with results from the four-antigen analysis. These data point to distinct peripheral FcR programming effects of IIV/FluZone and LAIV/FluMist.

Enhanced Fc-mediated antibody functions are elicited by LAIV/FluMist over IIV/FluZone

Given the observed differences in antibody titers and FcR binding responses across LAIV/FluMist and IIV/FluZone recipients, we next evaluated the Fc-effector profiles induced by these two distinct influenza vaccines. We first compared the fold changes of influenza-specific functional antibody activity across the two vaccines (Figure 4A). Specifically, we observed significantly enhanced antibody-dependent neutrophil phagocytosis (ADNP) and antibody-dependent complement deposition (ADCD) responses against antigens A_Singapore16_HA and B_Phuket13_HA in the IIV/FluZone vaccinees compared to the LAIV/FluMist recipients, consistent with the more significant enrichment of IgG1 and IgG3 binding to FcRs. However, unexpectedly, antibody-dependent monocyte phagocytosis (ADCP) and NK degranulation activity were enhanced in LAIV/FluMist recipients across antigens, including A_California09_HA and A_California09_NA, compared to IIV/FluZone

vaccinees. Therefore, here we observed a surprising pattern of enhanced FcR-dependent effector functions mediated by LAIV/FluMist over IIV/FluZone, across a panel of influenza antigens covering both influenza A and B strains and both HA and NA antigens.

These results further suggested that despite the quantitative advantages of those antibodies induced by IIV/FluZone vaccination, LAIV/FluMist vaccination may have promoted qualitatively superior influenza-specific antibodies. To test this overall hypothesis and to gain a better understanding of the functional quality, on a per antibody level, of the vaccine-induced humoral immune responses, antibody-dependent effector functional responses were normalized to the corresponding Influenza antigen-specific IgG titers at each time point (Figure 4B). According to this normalized analysis, functional antibody levels were significantly higher in LAIV/FluMist recipients across all functions against the A_California09_HA and A_California09_NA antigens. Also, significantly higher functional units for monocyte phagocytosis activity were also observed for the LAIV/FluMist group against A_Singapore16_HA, and the LAIV/FluMist-promoted NK cell activation was higher against B_Phuket13_HA. On the other hand, antibody-dependent complement deposition (ADCD) against B_Phuket13_HA was increased on a per-antibody level in the IIV/FluZone immunized individuals. Thus, these data suggest that while IIV/FluZone induced quantitively superior peripheral immune responses, LAIV/FluMist induced an overall qualitatively superior functional humoral immune response.

To gain a deeper understanding of overall architectural differences in the vaccine-induced immune response across the two vaccines, we constructed correlation matrices probing the relationships of isotype, subclass, and the FcR binding levels (x-axis) with antibody effector functions (y-axis) at Day 0 and Day 28 for both vaccines (Figure 4C). Strikingly, a nearly identical correlation structure was observed at baseline and following vaccination for individuals that received the IIV/FluZone vaccine, marked by the similar association profiles between IgG, IgA, and FcR-binding levels with ADCD and ADCP (Figure 4C, Top Row). Vaccination slightly but non-significantly improved the relationship between IgA1 and IgA2 with ADNK and ADNP and weakened the relationships of FcγRIIB binding levels and ADCP, marking small shifts in the types of antibody subpopulations available to drive the different antibody-Fc effector functions. These results collectively point to a relatively limited augmentation for an already established influenza-specific functional immune response induced by IIV/FluZone vaccination.

On the other hand, a marked shift in correlations was observed in the LAIV/FluMist cohort between pre- and post-immunizations (Figure 4C, Bottom Row). LAIV/FluMist promoted the emergence of robust novel correlations between A_California09_HA-specific total IgG1, A_California09_HA-specific FcγRIIA, and A_California09_HA-specific FcγRIIIA against all four A_California09_NA functions (ADCD, ADNK, ADNP, and ADCP). These results argue that in comparison to IIV/FluZone, despite the lack of a quantitative change in absolute antibody responses following the LAIV/FluMist vaccination, the LAIV/FluMist vaccine significantly alters the overall peripheral antibody architecture by inducing a more functionally active antigen-specific antibody repertoire.

Multivariate signatures of antibody responses across LAIV/FluMist and IIV/FluZone immune profiles point to qualitative and quantitative differences in vaccine-induced profiles.

Given the quantitative and qualitative differences observed at the univariate level across the IIV/FluZone and LAIV/FluMist vaccines, we next aimed to determine whether a multivariate signature may exist that is able to resolve the systematic antibody profiles promoted by the two vaccines. We first used a least absolute shrinkage and selection operator (LASSO) to define the minimal set of antibody features that could resolve the two vaccine responses, followed by a Partial Least Squares Discriminant Analysis (PLS-DA) to visualize the different responses (Figure 5A). Interestingly, a clear separation was observed across the two vaccine profiles with limited overlap between the Fc-antibody profiles. This separation was marked by a highly expanded subclass, isotype, and FcR binding responses in individuals that received IIV/FluZone, across largely the influenza A and some computationally designed antigens (Figure 5B). Conversely, an enrichment of functional antibody responses, with the higher NK cell, complement deposition, and neutrophil recruiting antibodies, in addition to IgA and IgG titers, were selectively expanded in individuals that received LAIV/FluMist. These analyses clearly highlight the induction of distinct humoral immune responses following the IIV/FluZone and LAIV/FluMist vaccination, marked by higher overall levels of the antibodies induced by IIV/FluZone and enhanced functional humoral immune responses induced by LAIV/FluMist.

LAIV/FluMist induced more coordinated functional profiles with preexisting antibodies.

Preexisting influenza-specific humoral immunity has been proposed to shape the breadth of the humoral immune response. These previous exposures may limit the breadth of humoral expansion towards new influenza strains and instead expand established memory cells, a process termed original antigenic sin (OAS) (28). To begin to probe the potential differential impact of OAS across the vaccine platforms, we examined the relationship between pre-existing humoral immune responses across the antigens and the vaccine-induced responses in individuals receiving the IIV/FluZone or LAIV/FluMist vaccine. We observed limited antagonism between pre-existing and post-vaccine-induced immune responses in LAIV/FluMist-vaccinated individuals (Figure 6A). Instead, we observed a robust correlation between most pre- and post-responses, even across A and B strains induced by the LAIV/FluMist vaccine. Meanwhile, the IIV/FluZone responses displayed relatively more limited correlations across all antigens, even marked by intermittent anti-correlated responses driven by features towards A_California09_HA and A_Brisbane07_HA (Figure 6B), pointing to enhanced vulnerability to OAS in the setting of IIV/FluZone vaccination compared to LAIV/FluMist. Finally, when the relationship across all antibody profile characteristics was assessed across LAIV/FluMist- and IIV/FluZone-induced immunity (Figure 6C–D), we observed more significant positive correlations in the LAIV/FluMist-associated immunity between the Fc-driven functions (ADCP and ADCD) and antibody titers (total IgG and IgG1) against the vaccine strains (A_California09_HA and A_California09_NA) when we compared the pre- and post-vaccination profiles (Figure 6C). Conversely, the IIV/FluZone-induced responses exhibited more correlations between antibody isotypes and subclasses with Fc receptor binding (Figure 6D). These results revealed enhanced coordination of

Fc-driven functions and antibody qualities induced by LAIV/FluMist vaccination, despite similar magnitudes and breadth of antibody titers compared to IIV/FluZone vaccination.

Discussion

Despite the recent decline in seasonal influenza incidence as a consequence of public health measures that were established globally during the COVID-19 pandemic, influenza remains an important public health concern owing to its persistent spread and the ever-present risk of future pandemics (29). However, current influenza vaccines provide variable and incomplete protection against the virus (30). Given our emerging appreciation for the role of the Fc-effector function in the protection against influenza viruses (5, 31), here we focused on exploring differences in the functional profiles of influenza-specific responses induced by the two approved influenza vaccines, FluMist and FluZone. Here, we report the presence of distinct antibody subclass levels, isotype titers, FcR binding, and functional responses across an expanded panel of influenza vaccine-associated antigens modulated by the live attenuated (LAIV/FluMist) and the inactivated (IIV/FluZone) seasonal influenza vaccines. Although the overall magnitude of the vaccine-induced immune responses was higher with the IIV/FluZone vaccination, LAIV/FluMist-induced qualitatively improved, non-neutralizing functional humoral immune responses. These results suggest that mucosal-targeted immunization may promote a more functionally optimized humoral immune response toward mucosal pathogens.

The HAI assay measures virus-specific neutralizing antibodies, and a relative HAI titer ratio of ≥40 is currently considered protective in adults. However, emerging data point to a critical role for several Fc-effector responses in the control and clearance of influenza and other respiratory pathogens (5). Specifically, opsinophagocytic, complement deposition, and NK cell activity have all been associated with protection against influenza both in animal models and humans (32). However, whether specific vaccine platforms are able to induce these extra-neutralizing functions more effectively remains unclear. Here, we observed a robust quantitative response induced by IIV/FluZone, linked to the enhanced FcR binding antibodies; however, these antibodies did not exhibit overall enhanced functional activity. Instead, LAIV/FluMist induced lower overall antibody titers and FcR binding but exhibited enhanced complement and NK cell functions to particular target antigens. Moreover, on a per antibody level, LAIV/FluMist induced functionally superior antibodies, suggesting that a mucosal, attenuated-virus priming strategy may generate superior antibodies compared to intramuscular split vaccine immunization towards influenza.

There are several limitations to this study. One inherent limitation of this study originates from the pre-existing variation in antibody responses and additional confounders such as age, gender, and previous vaccination history. It is important to illustrate whether the baseline properties of those individuals from the two subgroups may contribute to the differences in antibody responses observed in this work. Statistical analysis of those additional confounders revealed that the participants from the IIV/FluZone subgroup displayed a higher percentage of receiving the same influenza vaccination in the previous season as compared with those from the LAIV/FluMist subgroup. Therefore, some antibody responses observed in the IIV/FluZone subgroup may be disproportionally a “recall”

or “amnestic” response (33). However, we did not find evidence of a *de novo* affinity maturation in our LAIV/FluMist subjects as judged by the similar levels of IgM responses observed between the two subgroups. It is also unclear whether the observed differences here are being driven primarily by the site of delivery (intranasal vs. intramuscular) or the use of an attenuated virus instead of an inactivated virus. Other attenuated virus-based vaccines targeting respiratory pathogens such as the measles vaccine are routinely administered intramuscularly and provide durable protection. Moreover, whether these qualitative differences are indeed accompanied by superior functional antibodies in the respiratory mucosa is unknown. However, overall, these data point to nuanced peripheral antibody responses across two influenza vaccine platforms that may explain similar efficacy performance despite striking differences in peripheral antibody responses.

LAIV/FluMist has exhibited 80% efficacy in young children (<6 years old) and 40% efficacy in adults against matched strains (34). The efficacy has varied depending on studies, but the efficacy of LAIV/FluMist has been consistently higher in children (35). Moreover, LAIV/FluMist provides superior effectiveness over IIV/FluZone in young children (generally 70–90% against strains antigenically similar to the vaccine strains), and in recipients with a history of respiratory tract infections, asthma, and in HIV-positive patients (36). Additionally, LAIV/FluMist has been linked to attenuating the severity of disease in individuals who experience breakthrough infections (37). Thus, despite the lower antibody titers induced by LAIV/FluMist, it is plausible that the functionally optimized nature of the humoral immune response may contribute to the efficacy observed with this mucosal platform. Moreover, given that children mount more robust functional humoral immune responses following vaccination compared to adults (38). It is further possible that LAIV/FluMist drives a more robust response in children compared to adults, which may explain the higher efficacy observed in younger populations.

Anti-NA antibody titers correlate with a reduction in both viral shedding and infection severity, and small molecules that inhibit NA currently serve as critical therapeutics in the treatment of active influenza infections (10). While inhibition of NA activity has been postulated as a mechanism by which NA-antibodies may contribute to protection against influenza, NA-specific antibodies may also act via extra-neutralizing functions, similar to HA-specific ADCC-inducing antibodies (6). Moreover, given the more limited amino acid drift rates for NA and observed enhanced heterologous protection afforded by NA-specific antibodies (39), it is plausible that vaccines that can promote more effective NA functional immunity may contribute to enhanced global protection. We observed robust IgG1 and IgG3 responses to multiple NAs following IIV/FluZone vaccination; however, NA-specific NK cell function was higher in LAIV/FluMist vaccinated individuals, and the per antibody functional responses were largely higher in the LAIV/ FluMist immunized individuals. Similar to HA-specific antibodies, exposure to NA on a viral particle in the setting of LAIV/ FluMist may promote more targeted functional antibodies (40). The data here points to an important disconnection between the overall quantity and quality of the vaccine-induced humoral immune response that may be a key to protection against influenza.

Previous studies described the use of computationally optimized broadly reactive antigens (COBRA) for the development of HA- and NA-based broadly protective influenza vaccines.

The COBRA antigens, which incorporate epitopes based on the phylogenetic sequence of isolates and the corresponding timeframe and outbreaks (41), performed as a clear consensus on functional antibody performance to individual strains utilized across the studies. Specifically, we observed potent induction of binding antibodies to the COBRA antigens by both IIV/FluZone and LAIV/FluMist vaccination, albeit the responses were higher in IIV/FluZone vaccinees. However, COBRA-binding antibodies performed differently in our correlation evaluation, where a portion of COBRA-binding antibodies displayed a higher level of coordination across pre-existing and post-vaccine responses, suggesting that antibodies able to bind to these antigens may contribute to enhanced immunogenicity rather than blockade of the breadth of immunity.

Emerging data demonstrate that pre-existing antibodies rapidly capture vaccine antigens upon immunization, determining whether the antigen will be degraded and delivered to the lymph node to promote more effective immunity in an Fc-dependent manner (42, 43). Recent data pointed to an important role for FcγRIIB binding antibodies as a signature of more highly-adjuvanting pre-existing antibodies (42). Here, we observed the selective induction of FcγRIIB-binding antibodies with the LAIV/FluMist vaccine, which may drive enhanced delivery of antigen to lymph nodes, resulting in higher quality antibodies despite their lower quantitative levels. Moreover, the COBRA antigens may be captured by more adjuvant-like pre-existing antibodies that may be essential for promoting enhanced germinal center delivery, affinity maturation, and the evolution of breadth. Interestingly, certain COBRA antigens behaved differently across LAIV/FluMist and IIV/FluZone responses, where the A_X3_COBRA_HA appeared to antagonize the evolution of vaccine-induced immune responses in LAIV/FluMist-immunized individuals, pointing to the potential importance of antigen selection based on the platform.

Together, this study highlights several differences in the overall Fc profiles induced by IIV/FluZone and LAIV/FluMist vaccines. Future studies focused on profiling vaccine-induced immunity at the mucosa may provide further insights into the overall functional differences in immunity induced by these two vaccines and provide new insights on how these vaccines may be improved to drive enhanced immune protection against current and future influenza strains. However, most critically, the current study points to qualitative differences in vaccine-induced immune profiles that may be missed in vaccine development efforts that utilize strict quantitative binding and HAI to guide vaccine selection. Thus, coupled with our more sophisticated understanding of the mechanistic correlates of immunity against respiratory viruses (4, 44, 45), including influenza (1, 12, 46), next-generation vaccine development that probes the overall functional humoral and cellular immune response can lead to superior protection against this perpetually evolving virus.

Supplementary Material

Refer to Web version on PubMed Central for supplementary material.

Acknowledgments1

We thank Mark and Lisa Schwartz, Terry and Susan Ragon, and the SAMANA Kay MGH Research Scholars Award for their support. We also thank the University of Georgia Clinical and Translational Research Unit (CTRU) for its assistance. We thank all the volunteers in the UGA influenza vaccine studies that donated time and samples.

References

1. Krammer F 2019. The human antibody response to influenza A virus infection and vaccination. Nat Rev Immunol 19: 383–397. [PubMed: 30837674]
2. Zhang A, Stacey HD, Mullarkey CE, and Miller MS. 2019. Original Antigenic Sin: How First Exposure Shapes Lifelong Anti-Influenza Virus Immune Responses. J Immunol 202: 335–340. [PubMed: 30617114]
3. Chan L, Alizadeh K, Alizadeh K, Fazel F, Kakish JE, Karimi N, Knapp JP, Mehrani Y, Minott JA, Morovati S, Rghei A, Stegelmeier AA, Vanderkamp S, Karimi K, and Bridle BW. 2021. Review of Influenza Virus Vaccines: The Qualitative Nature of Immune Responses to Infection and Vaccination Is a Critical Consideration. Vaccines (Basel) 9: 972–979. [PubMed: 34579209]
4. Pantaleo G, Correia B, Fenwick C, Joo VS, and Perez L. 2022. Antibodies to combat viral infections: development strategies and progress. Nat Rev Drug Discov.
5. Boudreau CM, and Alter G. 2019. Extra-Neutralizing FcR-Mediated Antibody Functions for a Universal Influenza Vaccine. Front Immunol 10: 440–451. [PubMed: 30949165]
6. Rajendran M, Krammer F, and McMahon M. 2021. The Human Antibody Response to the Influenza Virus Neuraminidase Following Infection or Vaccination. Vaccines (Basel) 9: 437–454. [PubMed: 33946555]
7. Watanabe A, McCarthy KR, Kuraoka M, Schmidt AG, Adachi Y, Onodera T, Tonouchi K, Caradonna TM, Bajic G, Song S, McGee CE, Sempowski GD, Feng F, Urick P, Kepler TB, Takahashi Y, Harrison SC, and Kelsoe G. 2019. Antibodies to a Conserved Influenza Head Interface Epitope Protect by an IgG Subtype-Dependent Mechanism. Cell 177: 1124–1135 e1116. [PubMed: 31100267]
8. Wang X, Li Y, O'Brien KL, Madhi SA, Widdowson MA, Byass P, Omer SB, Abbas Q, Ali A, Amu A, Azziz-Baumgartner E, Bassat Q, Abdullah Brooks W, Chaves SS, Chung A, Cohen C, Echavarria M, Fasce RA, Gentile A, Gordon A, Groome M, Heikkinen T, Hirve S, Jara JH, Katz MA, Khuri-Bulos N, Krishnan A, de Leon O, Lucero MG, McCracken JP, Mira-Iglesias A, Moisi JC, Munywoki PK, Ourohire M, Polack FP, Rahi M, Rasmussen ZA, Rath BA, Saha SK, Simoes EA, Sotomayor V, Thamthitiwat S, Treurnicht FK, Wamukoya M, Yoshida LM, Zar HJ, Campbell H, Nair H, and Respiratory N Virus Global Epidemiology. 2020. Global burden of respiratory infections associated with seasonal influenza in children under 5 years in 2018: a systematic review and modelling study. Lancet Glob Health 8: e497–e510. [PubMed: 32087815]
9. Clements ML, and Murphy BR. 1986. Development and persistence of local and systemic antibody responses in adults given live attenuated or inactivated influenza A virus vaccine. J Clin Microbiol 23: 66–72. [PubMed: 3700610]
10. He W, Tan GS, Mullarkey CE, Lee AJ, Lam MM, Krammer F, Henry C, Wilson PC, Ashkar AA, Palese P, and Miller MS. 2016. Epitope specificity plays a critical role in regulating antibody-dependent cell-mediated cytotoxicity against influenza A virus. Proc Natl Acad Sci U S A 113: 11931–11936. [PubMed: 27698132]
11. Beyer WE, Palache AM, de Jong JC, and Osterhaus AD. 2002. Cold-adapted live influenza vaccine versus inactivated vaccine: systemic vaccine reactions, local and systemic antibody response, and vaccine efficacy. A meta-analysis. Vaccine 20: 1340–1353. [PubMed: 11818152]
12. Boudreau CM, Yu WH, Suscovich TJ, Talbot HK, Edwards KM, and Alter G. 2020. Selective induction of antibody effector functional responses using MF59-adjuvanted vaccination. J Clin Invest 130: 662–672. [PubMed: 31845904]
13. Wu S, Ross TM, Carlock MA, Ghedin E, Choi H, and Vogel C. 2022. Evaluation of determinants of the serological response to the quadrivalent split-inactivated influenza vaccine. Mol Syst Biol 18: e10724: 1012–1023.

14. Brown EP, Dowell KG, Boesch AW, Normandin E, Mahan AE, Chu T, Barouch DH, Bailey-Kellogg C, Alter G, and Ackerman ME. 2017. Multiplexed Fc array for evaluation of antigen-specific antibody effector profiles. J Immunol Methods 443: 33–44. [PubMed: 28163018]
15. Brown EP, Licht AF, Dugast AS, Choi I, Bailey-Kellogg C, Alter G, and Ackerman ME. 2012. High-throughput, multiplexed IgG subclassing of antigen-specific antibodies from clinical samples. J Immunol Methods 386: 117–123. [PubMed: 23023091]
16. Ackerman ME, Moldt B, Wyatt RT, Dugast AS, McAndrew E, Tsoukas S, Jost S, Berger CT, Sciaranghella G, Liu Q, Irvine DJ, Burton DR, and Alter G. 2011. A robust, high-throughput assay to determine the phagocytic activity of clinical antibody samples. J Immunol Methods 366: 8–19. [PubMed: 21192942]
17. Karsten CB, Mehta N, Shin SA, Diefenbach TJ, Slein MD, Karpinski W, Irvine EB, Broge T, Suscovich TJ, and Alter G. 2019. A versatile high-throughput assay to characterize antibody-mediated neutrophil phagocytosis. J Immunol Methods 471: 46–56. [PubMed: 31132351]
18. Fischinger S, Fallon JK, Michell AR, Broge T, Suscovich TJ, Streeck H, and Alter G. 2019. A high-throughput, bead-based, antigen-specific assay to assess the ability of antibodies to induce complement activation. J Immunol Methods 473: 112630–112642. [PubMed: 31301278]
19. Jegaskanda S, Vanderven HA, Tan HX, Alcantara S, Wragg KM, Parsons MS, Chung AW, Juno JA, and Kent SJ. 2019. Influenza Virus Infection Enhances Antibody-Mediated NK Cell Functions via Type I Interferon-Dependent Pathways. J Virol 93: 42–47.
20. Jegaskanda S, Weinfurter JT, Friedrich TC, and Kent SJ. 2013. Antibody-dependent cellular cytotoxicity is associated with control of pandemic H1N1 influenza virus infection of macaques. J Virol 87: 5512–5522. [PubMed: 23468501]
21. Huber VC, Lynch JM, Bucher DJ, Le J, and Metzger DW. 2001. Fc receptor-mediated phagocytosis makes a significant contribution to clearance of influenza virus infections. J Immunol 166: 7381–7388. [PubMed: 11390489]
22. Huang Y, França MS, Allen JD, Shi H, and Ross TM. 2021. Next Generation of Computationally Optimized Broadly Reactive HA Vaccines Elicited Cross-Reactive Immune Responses and Provided Protection against H1N1 Virus Infection. Vaccines (Basel) 9: 32–38. [PubMed: 33435566]
23. Sautto GA, Kirchenbaum GA, Abreu RB, Ecker JW, Pierce SR, Kleanthous H, and Ross TM. 2020. A Computationally Optimized Broadly Reactive Antigen Subtype-Specific Influenza Vaccine Strategy Elicits Unique Potent Broadly Neutralizing Antibodies against Hemagglutinin. J Immunol 204: 375–385. [PubMed: 31811019]
24. Giles BM, and Ross TM. 2011. A computationally optimized broadly reactive antigen (COBRA) based H5N1 VLP vaccine elicits broadly reactive antibodies in mice and ferrets. Vaccine 29: 3043–3054. [PubMed: 21320540]
25. Carter DM, Darby CA, Lefoley BC, Crevar CJ, Alefantis T, Oomen R, Anderson SF, Strugnell T, Cortés-Garcia G, Vogel TU, Parrington M, Kleanthous H, and Ross TM. 2016. Design and Characterization of a Computationally Optimized Broadly Reactive Hemagglutinin Vaccine for H1N1 Influenza Viruses. J Virol 90: 4720–4734. [PubMed: 26912624]
26. Wong TM, Allen JD, Bebin-Blackwell AG, Carter DM, Alefantis T, DiNapoli J, Kleanthous H, and Ross TM. 2017. Computationally Optimized Broadly Reactive Hemagglutinin Elicits Hemagglutination Inhibition Antibodies against a Panel of H3N2 Influenza Virus Cocirculating Variants. J Virol 91: 2–11.
27. Giles BM, Crevar CJ, Carter DM, Bissel SJ, Schultz-Cherry S, Wiley CA, and Ross TM. 2012. A computationally optimized hemagglutinin virus-like particle vaccine elicits broadly reactive antibodies that protect nonhuman primates from H5N1 infection. J Infect Dis 205: 1562–1570. [PubMed: 22448011]
28. Chromikova V, Tan J, Aslam S, Rajabhathor A, Bermudez-Gonzalez M, Ayllon J, Simon V, Garcia-Sastre A, Salaun B, Nachbagauer R, and Krammer F. 2020. Activity of human serum antibodies in an influenza virus hemagglutinin stalk-based ADCC reporter assay correlates with activity in a CD107a degranulation assay. Vaccine 38: 1953–1961. [PubMed: 31959425]
29. Zhou G, and Zhao Q. 2020. Perspectives on therapeutic neutralizing antibodies against the Novel Coronavirus SARS-CoV-2. Int J Biol Sci 16: 1718–1723. [PubMed: 32226289]

30. Breteler JK, Tam JS, Jit M, Ket JC, and De Boer MR. 2013. Efficacy and effectiveness of seasonal and pandemic A (H1N1) 2009 influenza vaccines in low and middle income countries: a systematic review and meta-analysis. Vaccine 31: 5168–5177. [PubMed: 24012574]

31. Yang J, Zhang J, Han T, Liu C, Li X, Yan L, Yang B, and Yang X. 2020. Effectiveness, immunogenicity, and safety of influenza vaccines with MF59 adjuvant in healthy people of different age groups: A systematic review and meta-analysis. Medicine (Baltimore) 99: e19095: 22–28.

32. Jennewein MF, Goldfarb I, Dolatshahi S, Cosgrove C, Noelette FJ, Krykbaeva M, Das J, Sarkar A, Gorman MJ, Fischinger S, Boudreau CM, Brown J, Cooperrider JH, Aneja J, Suscovich TJ, Graham BS, Lauer GM, Goetghebuer T, Marchant A, Lauffenburger D, Kim AY, Riley LE, and Alter G. 2019. Fc Glycan-Mediated Regulation of Placental Antibody Transfer. Cell 178: 202–215 e214. [PubMed: 31204102]

33. McNamara RP, Maron JS, Boucau J, Roy V, Webb NE, Bertera HL, Barczak AK, Positives Study Staff T, Franko N, Logue JK, Kemp M, Li JZ, Zhou L, Hsieh CL, McLellan JS, Siedner MJ, Seaman MS, Lemieux JE, Chu HY, and Alter G. 2023. Anamnestic humoral correlates of immunity across SARS-CoV-2 variants of concern. mBio 14: e0090223: 11–21.

34. Rondy M, El Omeiri N, Thompson MG, Leveque A, Moren A, and Sullivan SG. 2017. Effectiveness of influenza vaccines in preventing severe influenza illness among adults: A systematic review and meta-analysis of test-negative design case-control studies. J Infect 75: 381–394. [PubMed: 28935236]

35. Vanderven HA, Liu L, Ana-Sosa-Batiz F, Nguyen TH, Wan Y, Wines B, Hogarth PM, Tilmanis D, Reynaldi A, Parsons MS, Hurt AC, Davenport MP, Kotsimbos T, Cheng AC, Kedzierska K, Zhang X, Xu J, and Kent SJ. 2017. Fc functional antibodies in humans with severe H7N9 and seasonal influenza. JCI Insight 2: 2–18.

36. DiazGranados CA, Dunning AJ, Kimmel M, Kirby D, Treanor J, Collins A, Pollak R, Christoff J, Earl J, Landolfi V, Martin E, Gurunathan S, Nathan R, Greenberg DP, Tornieporth NG, Decker MD, and Talbot HK. 2014. Efficacy of high-dose versus standard-dose influenza vaccine in older adults. N Engl J Med 371: 635–645. [PubMed: 25119609]

37. Puig-Barbera J, Tamames-Gomez S, Plans-Rubio P, and Eiros-Bouza JM. 2022. Relative Effectiveness of Cell-Cultured versus Egg-Based Seasonal Influenza Vaccines in Preventing Influenza-Related Outcomes in Subjects 18 Years Old or Older: A Systematic Review and Meta-Analysis. Int J Environ Res Public Health 19.

38. Bartsch YC, St Denis KJ, Kaplonek P, Kang J, Lam EC, Burns MD, Farkas EJ, Davis JP, Boribong BP, Edlow AG, Fasano A, Shreffler WG, Zavadska D, Johnson M, Goldblatt D, Balazs AB, Yonker LM, and Alter G. 2022. SARS-CoV-2 mRNA vaccination elicits robust antibody responses in children. Sci Transl Med: eabn9237: 128–136.

39. Stadlbauer D, Zhu X, McMahon M, Turner JS, Wohlbold TJ, Schmitz AJ, Strohmeier S, Yu W, Nachbagauer R, Mudd PA, Wilson IA, Ellebedy AH, and Krammer F. 2019. Broadly protective human antibodies that target the active site of influenza virus neuraminidase. Science 366: 499–504. [PubMed: 31649200]

40. Strohmeier S, Amanat F, Carreno JM, and Krammer F. 2022. Monoclonal antibodies targeting the influenza virus N6 neuraminidase. Front Immunol 13: 944907–944920. [PubMed: 35967389]

41. Ackerman ME, Crispin M, Yu X, Baruah K, Boesch AW, Harvey DJ, Dugast AS, Heizen EL, Ercan A, Choi I, Streeck H, Nigrovic PA, Bailey-Kellogg C, Scanlan C, and Alter G. 2013. Natural variation in Fc glycosylation of HIV-specific antibodies impacts antiviral activity. J Clin Invest 123: 2183–2192. [PubMed: 23563315]

42. Lofano G, Gorman MJ, Yousif AS, Yu WH, Fox JM, Dugast AS, Ackerman ME, Suscovich TJ, Weiner J, Barouch D, Streeck H, Little S, Smith D, Richman D, Lauffenburger D, Walker BD, Diamond MS, and Alter G. 2018. Antigen-specific antibody Fc glycosylation enhances humoral immunity via the recruitment of complement. Sci Immunol 3: 32–39.

43. Wang TT, Maamary J, Tan GS, Bournazos S, Davis CW, Krammer F, Schlesinger SJ, Palese P, Ahmed R, and Ravetch JV. 2015. Anti-HA Glycoforms Drive B Cell Affinity Selection and Determine Influenza Vaccine Efficacy. Cell 162: 160–169. [PubMed: 26140596]

44. Battles MB, and McLellan JS. 2019. Respiratory syncytial virus entry and how to block it. Nat Rev Microbiol 17: 233–245. [PubMed: 30723301]

45. Abernathy ME, Dam KA, Esswein SR, Jette CA, and Bjorkman PJ. 2021. How Antibodies Recognize Pathogenic Viruses: Structural Correlates of Antibody Neutralization of HIV-1, SARS-CoV-2, and Zika. Viruses 13: 138–146. [PubMed: 33478104]

46. Wei CJ, Crank MC, Shiver J, Graham BS, Mascola JR, and Nabel GJ. 2020. Next-generation influenza vaccines: opportunities and challenges. Nat Rev Drug Discov 19: 239–252. [PubMed: 32060419]

Key points:

1. FluZone and FluMist induced broadly different functional humoral profiles.
2. FluZone induced superior antibody titer and Fcγ-receptor binding than FluMist.
3. FluMist induced a more robust functional humoral response than FluZone.

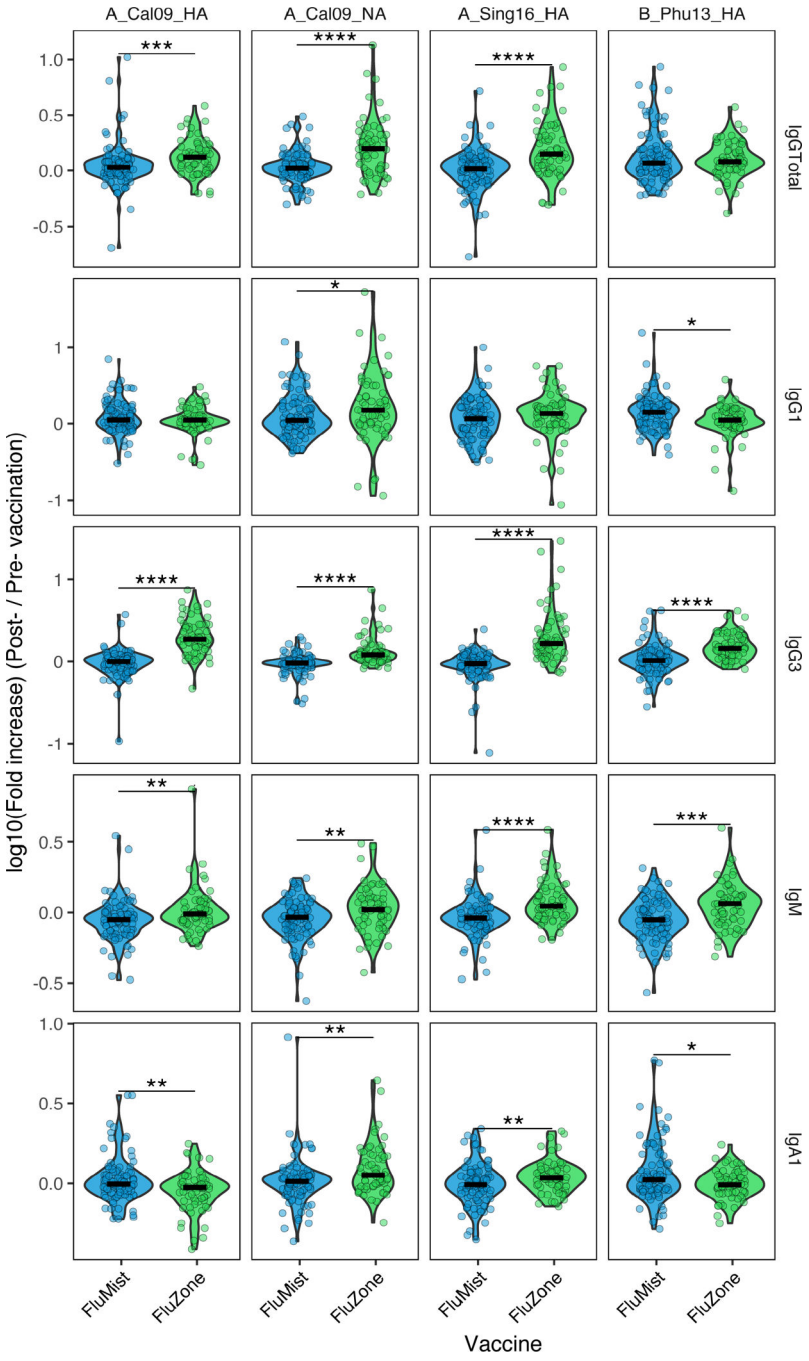

Fig. 1.

Vaccine-mediated antibody responses against common influenza antigens differ between LAIV/FluMist and IIV/FluZone vaccinees. The levels of fold increase in antibody titers of total IgG, IgG1, IgG3, IgA1, and IgM specifically induced by each vaccination against the four influenza antigens (A_California09_HA, A_California09_NA, A_Singapore16_HA, and B_Phuket13_HA) and one negative control antigen (Ebola Glycoprotein) were quantified through Luminex assays with serum samples of LAIV/FluMist (n = 93) and IIV/FluZone (n = 63) vaccinees. The specific fold increase was presented as log10 value of

the post- (Day 28)/pre- (Day 0) vaccination. Fold increases that significantly differ between Day 0 and Day 28 are marked with asterisk symbols of LAIV/FluMist (blue) and IIV/FluZone (green) subgroups. Asterisks indicate statistically significant correlations; *p≤0.05, **p≤0.01, ***p≤0.001, ****p≤0.0001. See Gating Strategy in Fig. S1 for antigen-specific gating.

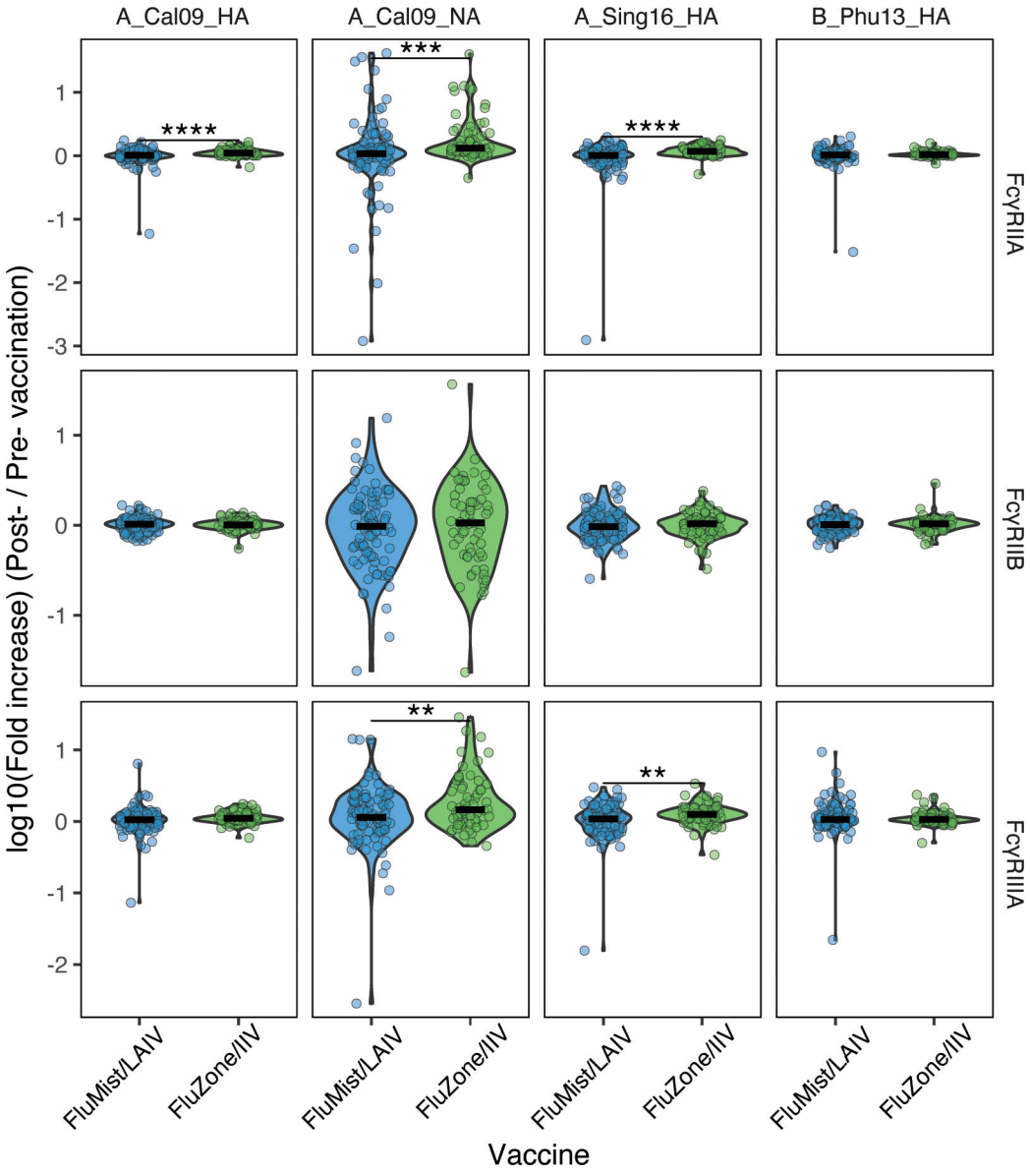

Fig. 2.

IIV/FluZone induced a more significant enhancement in FcγR-binding antibodies than LAIV/FluMist against four common influenza antigens (A_California09_HA, A_California09_NA, A_Singapore16_HA, and B_Phuket13_HA) and one control antigen (Ebola Glycoprotein). The levels of fold increase in binding capacity of the vaccine-induced antibodies towards FcgRIIA, FcgRIIB, and FcgRIIIA were quantified via Luminex assays with serum samples of LAIV/FluMist (n = 93) and IIV/FluZone (n = 63) vaccinees. The specific fold increase was presented as log10 value of the post- (Day 28)/pre- (Day 0) vaccination. Fold increases that significantly differ between Day 0 and Day 28 are marked with asterisk symbols of LAIV/FluMist (blue) and IIV/FluZone (green) subgroups. Asterisks indicate statistically significant correlations; *p≤0.05, **p≤0.01, ***p≤0.001, ****p≤0.0001. See Gating Strategy in Fig. S1 for antigen-specific gating.

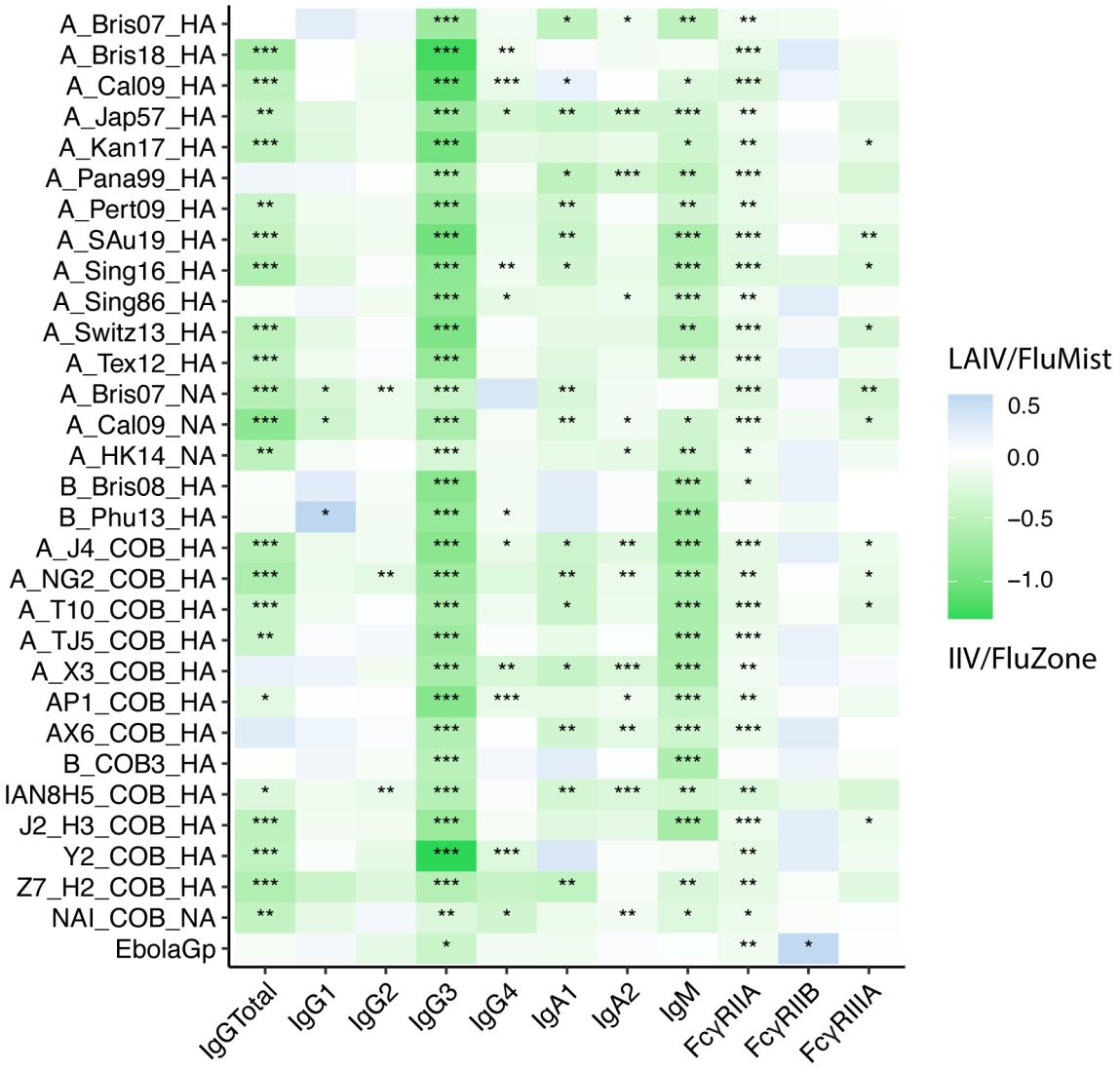

Fig. 3.

Enrichment heatmap showing the overall comparison of fold-change in antibody levels and FcγR-binding profiles induced by IIV/FluZone and LAIV/FluMist. Heatmap represents the difference in median delta values between the LAIV/FluMist - and IIV/FluZone -induced antibody responses of total IgG, IgG1, IgG2, IgG3, IgG4, IgA1, IgA2, IgM, FcγRIIA, FcγRIIB, and FcγRIIIA against an expanded set of influenza antigens. Each measurement is z-scored for later subtraction. Each z score value represents the number of standard deviations by which the value of the raw Luminex MFI values assayed here is above or below the mean value of data points in each subgroup. Raw values above the mean have positive z scores, while those below the mean have negative z scores. It is calculated by subtracting the population mean from an individual raw score and then dividing the difference by the population standard deviation. The enriched group is indicated by the color key for IIV/FluZone (green) and LAIV/FluMist (blue). Asterisks indicate statistically significant correlations; *p≤0.05, **p≤0.01, ***p≤0.001, ****p≤0.0001. See Gating Strategy in Fig. S1 for antigen-specific gating.

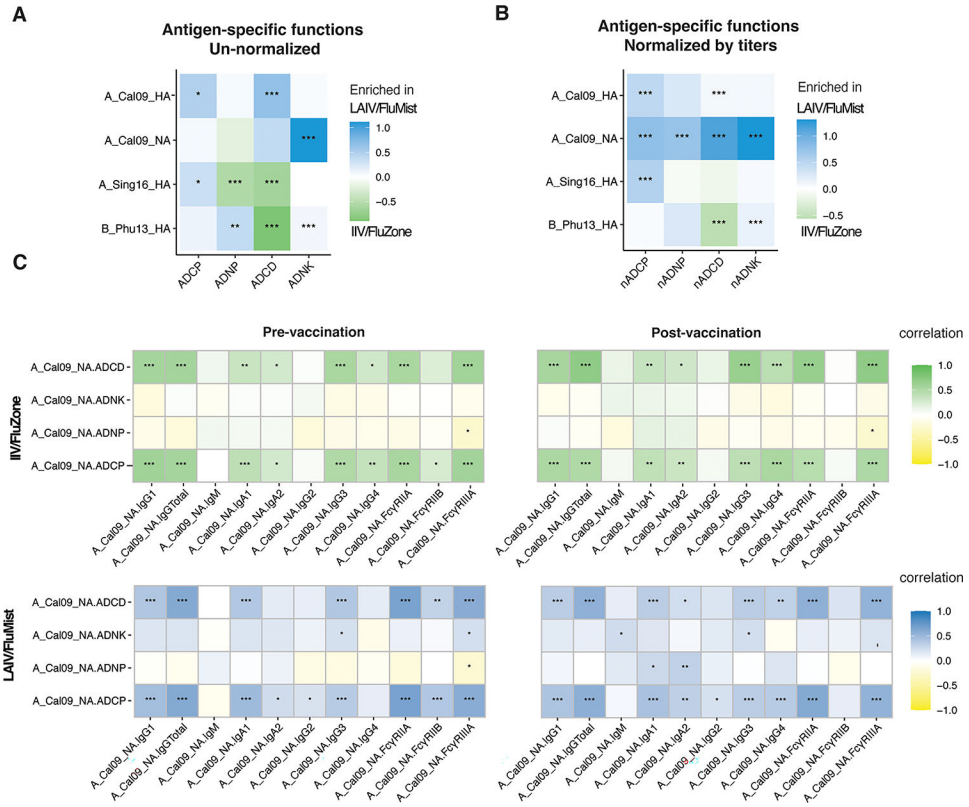

Fig. 4.

FluMist improves the functional breadth of anti-influenza antibody effector responses. (A) Heatmap represents the mean delta values between the FluMist- and FluZone-induced functional immunity for ADCP, ADNP, ADCD, and ADNK against A_California09_HA, A_California09_NA, A_Singapore16_HA, and B_Phuket13_HA. (B) Heatmap shows the mean delta values between the LAIV/FluMist- and IIV/FluZone-induced functional immunity normalized to the corresponding total IgG titers. (C) Heatmaps show Spearman correlations between LAIV/FluMist (top row) and IIV/FluZone (bottom row) antibody effector functions corresponding to antibody titers and FcγRs binding. The colors indicate the correlation coefficient (r) as indicated by the color key for IIV/FluZone (green) and LAIV/FluMist (blue). Asterisks indicate statistically significant correlations; *p≤0.05, **p≤0.01, ***p≤0.001, ****p≤0.0001. See Gating Strategy in Fig. S1 for antigens specific gating, ADCD, ADNP, ADCP, and ADNKA measurements.

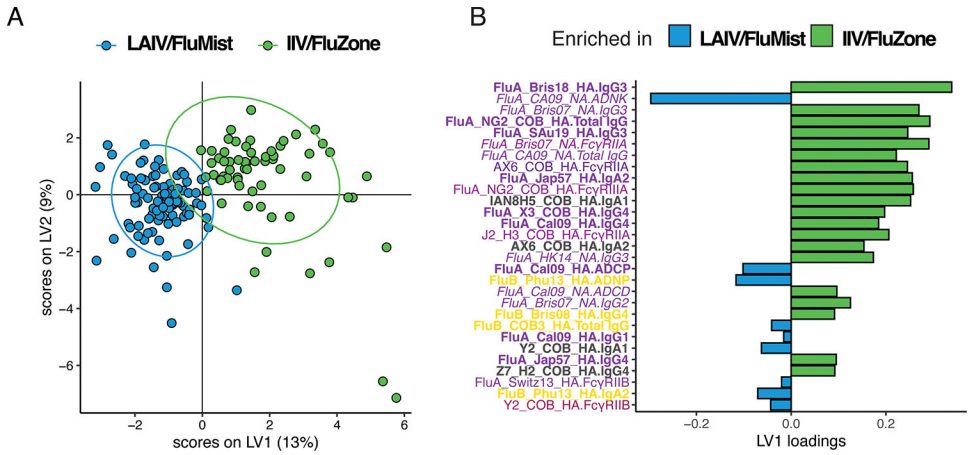

Fig. 5.

Multivariate analysis of humoral antibody responses promoted by FluMist and FluZone. Computational modeling was applied to distinguish features enhanced following vaccination. (A) LASSO Partial Least Squares Discriminant Analysis (LASSO-PLSDA) of influenza-specific antibody features between FluMist and FluZone orthogonalized on the latent variable 1 (LV1). LV1 explains 13% of the variance along the X-axis while LV2 explains 9% of the variance along the Y-axis. (B) The Variable Importance in Projection (VIP) scores for the PLSDA indicate the prime factors driving the differences between the LAIV/FluMist (blue) and IIV/FluZone (green) samples. Parameters pointing toward the left are enriched in LAIV/FluMist samples, while those pointing right are enriched in IIV/FluZone samples. Bar color and length correspond to relative importance. Antibody features are colored by category.

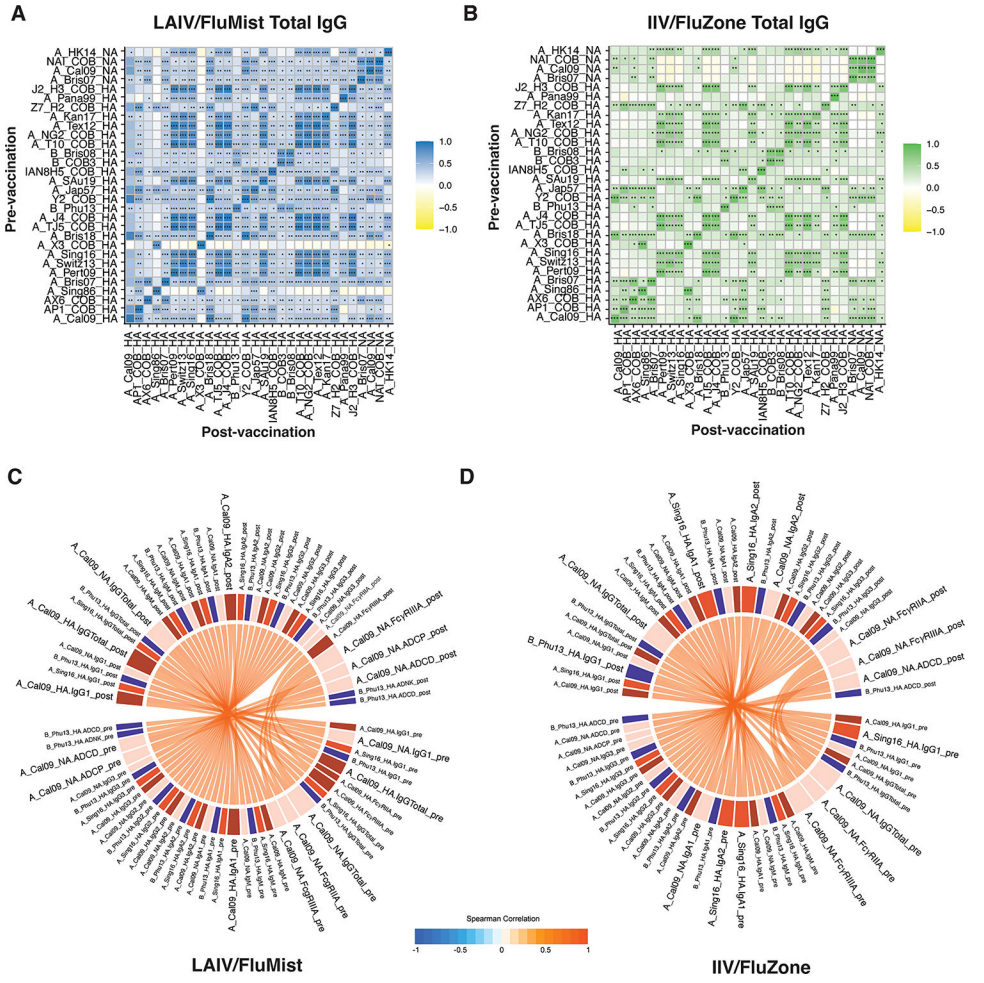

Fig 6.

LAIV/FluMist induced more significant and coordinated Fc-effector function, but not antibody titers and binding to Fcγ-Receptors between the pre-vaccination and post-vaccination time points. Correlation heatmaps show pairwise Spearman correlation matrices of antigen-specific between pre- vs. post-vaccination measurements for LAIV/FluMist (**A**) and IIV/FluZone **(B)**. Negative correlations are indicated in yellow, and positive correlations are denoted in green for IIV/FluZone and blue for LAIV/FluMist. Statistical significance is indicated by asterisks with Holm-Bonferroni correction for multiple hypothesis testing; *p≤0.05, **p≤0.01, ***p≤0.001, ****p≤0.0001. (**C-D**) Chord diagrams show Spearman correlations between pre- and post-vaccination features of LAIV/FluMist (**C**) and IIV/FluZone (**D**). Spearman correlations are links that carry the color of the average correlation coefficient between pre- and post-vaccination measurements. The arc length of each segment is automatically scaled to the number of correlating segments it pairs with. Only positive corrections (denoted by red connectors) with an absolute value of correlation > 0.95 and p-value < 0.0001 are recorded here. See Gating Strategy in Fig. S1 for antigens-specific gating, ADCD, ADNP, ADCP, and ADNK measurements.

Table 1:

Statistical analyses of demographic characteristics of LAIV/FluMist and IIV/FluZone

	LAIV/FluMist (n= 94)	IIV/FluZone (n = 63)	Statistical Analyses	
Gender			**Fisher's Exact Test, P value**	**Statistically significant (P < 0.05)?**
Male, n (%)	32 (34.0%)	22 (34.9%)	>0.9999	No
Female, n (%)	62 (66.0%)	41 (65.1%)		
Age			**Mann Whitney Test, P value**	**Statistically significant (P < 0.05)?**
Median (Range)	26 (18–49)	28 (20–51)	>0.9999	No
BMI			**Mann Whitney Test, P value**	**Statistically significant (P < 0.05)?**
Median (Range)	25.20 (18.2–60.7)	25.94 (18.2–42.1)	>0.9999	No
Race/Ethnicity			**Chi Square Test, P value**	**Statistically significant (P < 0.05)?"**
White/Caucasian	67 (71.3%)	51 (81%)	0.0378 *	Yes
African American	17 (18.1%)	2 (3.1%)		
Hispanic/Latino	6 (6.4%)	7 (11.0%)		
Asian	4 (4.3%)	3 (4.8%)		
Vaccination in the previous season (2017–2018)			**Fisher's Exact Test, P value**	**Statistically significant (P < 0.05)?"**
Vaccinated	69 (73.4%)	60 (95.2%)	0.0005 ***	Yes
Not Vaccinated	25 (26.6%)	3 (4.8%)		

[1]Univariate analysis of demographic characteristics, including age, BMI, gender, race/ethnicity, and previous history of influenza vaccination (2017-2018), between the LAIV/FluMist and IIV/FluZone subgroups. Asterisks indicate statistically significant variations;

*p≤0.05,

**p≤0.01,

***p≤0.001,

****p≤0.0001. Fisher's Exact Test, Mann Whitney Test, and Chi Square Test were applied for the calculation of P values.